J Biomol NMR (2014) 58:149–154
DOI 10.1007/s10858-014-9817-3

COMMUNICATION

A decadentate Gd(III)-coordinating paramagnetic cosolvent for protein relaxation enhancement measurement

Xin-Hua Gu · Zhou Gong · Da-Chuan Guo · Wei-Ping Zhang · Chun Tang

Received: 27 November 2013 / Accepted: 31 January 2014 / Published online: 9 February 2014

Abstract Solvent paramagnetic relaxation enhancement (sPRE) arises from random collisions between paramagnetic cosolvent and protein of interest. The sPRE can be readily measured, affording protein structure information. However, lack of an inert cosolvent probe may yield sPRE values that are not consistent with protein structure. Here we synthesized a new sPRE probe, triethylenetetraamine hexaacetate trimethylamide gadolinium, or Gd(III)–TTHA–TMA. With a total of 10 coordination sites, this paramagnetic cosovlent eliminates an inner-sphere water molecule that can otherwise transfer relaxation to protein through exchange. With the metal ion centered, the new probe is largely spherical with a radius of 4.0 Å, permitting accurate back calculation of sPRE. The effectiveness Gd(III)–TTHA–TMA as a sPRE probe was demonstrated on three well-studied protein systems.

Keywords NMR spectroscopy · Protein structures · Paramagnetic relaxation enhancement · Paramagnetic probe · Solvent PRE

Xin-Hua Gu and Zhou Gong have contributed equally to this article.

Electronic supplementary material The online version of this article (doi:10.1007/s10858-014-9817-3) contains supplementary material, which is available to authorized users.

X.-H. Gu · Z. Gong · D.-C. Guo · C. Tang (✉)
State Key Laboratory of Magnetic Resonance and Atomic Molecular Physics and Wuhan Institute of Physics and Mathematics, Chinese Academy of Sciences, Wuhan 430071, Hubei Province, China
e-mail: tanglab@wipm.ac.cn

W.-P. Zhang (✉)
Department of Pharmacology, Zhejiang University School of Medicine, Hangzhou, Zhejiang Province, China
e-mail: weiping601@zju.edu.cn

Protein structure determination by solution NMR has gone from solely NOE-based (Wüthrich 1986) to an integrative approach (Schwieters et al. 2006; Karaca and Bonvin 2013), as incorporation of different types of experimental restraints yields protein structures of better precision and accuracy. Among those techniques, paramagnetic relaxation enhancement (PRE) affords distance measurements up to 40 Å between the paramagnetic probe introduced at a desired site and protein nuclei (Iwahara et al. 2004; Clore and Iwahara 2009; Otting 2010). In recent years, PRE has been used for structure determination of protein complexes (Mal et al. 2002; Keizers et al. 2010), membrane proteins (Berardi et al. 2011; Gottstein et al. 2012; Klammt et al. 2012) and intrinsically disordered proteins (Gillespie and Shortle 1997; Eliezer 2012). However, introduction of a paramagnetic probe, either through chemical conjugation to a specific cysteine residue or by protein engineering, may inadvertently perturb protein structure and function.

Solvent PRE (sPRE) arises from random collisions between a paramagnetic cosolvent and protein of interest. Several types of paramagnetic cosolvents have been used previously, including pressurized molecular oxygen (Hernandez et al. 2002), 4-hydroxy-2,2,6,6-tetramethylpiperidinyl-1-oxy (TEMPOL) (Petros et al. 1990; Venditti et al. 2008), and diethylenetriamine pentaacetate bismethylamide gadolinium chelate (Gd(III)–DTPA–BMA) (Pintacuda and Otting 2002; Iwahara et al. 2006; Madl et al. 2009, 2011). Surrounded by the paramagnetic cosolvent, residues close to the protein surface experience larger sPRE than the residues more deeply buried. As such, sPRE measurement provides distance information about the relative depth of a nucleus in a protein (Wang et al. 2012), and it has been used for structure determination of small to medium sized proteins (Madl et al. 2009) as well as protein–protein complexes (Madl et al. 2011). Comparing to the PRE measurement with a covalently conjugated paramagnetic

probe, sPRE restraints can be readily obtained and used in combination with other types of NMR and biophysical restraints for structure determination (Koehler and Meiler 2011; Karaca and Bonvin 2013).

Among the paramagnetic cosolvents used for sPRE measurement, Gd(III)–DTPA–BMA probe has been most popular (Bernini et al. 2009), and has been incorporated to characterize individual proteins (Pintacuda and Otting 2002; Madl et al. 2009), protein–protein complexes (Guttler et al. 2010; Madl et al. 2011) and protein-DNA complexes (Iwahara et al. 2006). Gd(III)–DTPA–BMA is nonpolar and carries no net charge, hence it does not specifically interact with the protein of interest (Pintacuda and Otting 2002). Also known under trade name Omniscan, Gd(III)–DTPA–BMA is widely used in magnetic resonance imaging (MRI). As a contrasting agent, DTPA–BMA provides only 8 coordinate sites to Gd(III), with the 9th coordination site provided by an inner-sphere water molecule (Fig. 1), thus enhancing the relaxation of bulk water through exchange. When used for sPRE measurement, water relaxation can in turn be transferred to protein nuclei, in particular to those labile non-hydrogen-bonded protons. Indeed, solvent-transferred PRE gave rise to extremely large PRE values for amide protons of $\sim$25 residues in maltose-binding protein (MBP), as acknowledged by the authors (Fig. S1) (Madl et al. 2009). Measurement of sPRE values for ^{13}C-bonded non-labile protons of MBP, however, only partially alleviated the problem, with large sPRE values still visible for residues Val246, Lys251, Gly252, Asn272, and Leu275 (Madl et al. 2009).

In our hands, with Gd(III)–DTPA–BMA cosolvent added to protein GB1, we observed sPRE values much larger with addition of 4 mM cosovlent, than the calculated values based on the protein structure (Gronenborn et al. 1991; Derrick and Wigley 1994). GB1, the immunoglobulin-binding domain of streptococcal protein G, is a commonly used model protein in NMR. In this 56-residue globular protein, Glu43, a sheet residue with amide proton pointing outwards and Glu56, the C-terminal residue, are both broadened out beyond detection. Thr2, a residue near the protein N-terminus, and Ala23, a residue at one end of a helix, both experience sPRE values much larger than the calculated (Fig. S2). Excluding those residues that have disappeared, the correlation coefficient between observed and calculated sPRE values is 0.71. As such, using Gd(III)–DTPA–BMA as the paramagnetic cosolvent, the measured sPRE value can deviate from the assumed distance dependency on the depth of the nucleus, which would introduce systematic errors when used for protein structure calculation.

Inspired by the usefulness of DTPA–BMA in measuring sPRE, and with the goal to eliminate the water exchange problem, we designed and synthesized a new paramagnetic cosolvent, triethylenetetraamine hexaacetate trimethylamide gadolinium chelate (Gd(III)–TTHA–TMA, Fig. 1). The cosolvent was synthesized in just two steps, starting from commercially available triethyleneteraamine hexaacetic acid (TTHA, Scheme 1), reacted with methylamine hydrochloride and Gd(III) oxide sequentially. The resulted product can be purified through both cation and anion exchange columns. Similar to Gd(III)–DTPA–BMA, Gd(III)–TTHA–TMA is non-polar and carries no net charge. With an extra arm of carboxylate amide, the new probe provides a total of 10 coordination sites, completely wrapping the gadolinium ion inside (Fig. 1) and affording a metal-centered sphere with a $\sim$4.0 Å radius (Fig. S3). In contrast, Gd(III)–DTPA–BMA is shaped like a bowl, with the radius from the metal center varying from 3.0 to 4.5 Å (Fig. S3). As a small molecule, Gd(III)–DTPA–BMA can rotate much more rapidly than the protein under investigation. However, depending on which side of the probe that approaches and collides with the protein, different sPRE values can be resulted owing to different metal-proton distance. The irregular shape of Gd(III)–DTPA–BMA probe cannot be properly treated in a grid model, and for the back-calculation of sPRE values an average radius of 3.5 Å has been assumed (Hernandez et al. 2002; Pintacuda and Otting 2002; Madl et al. 2009).

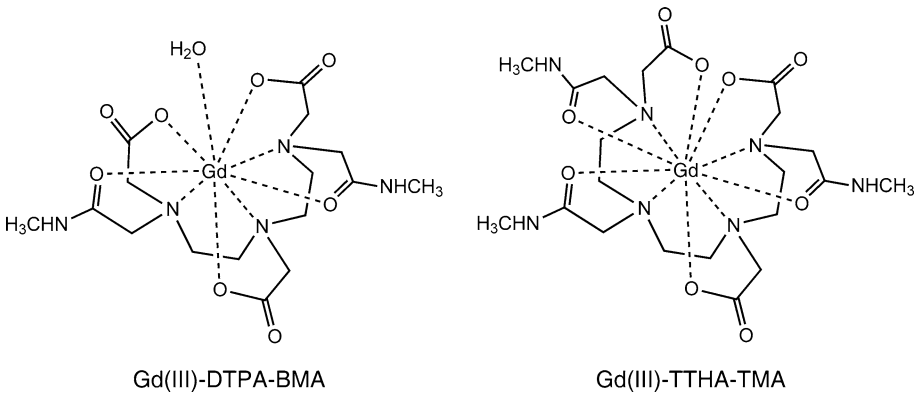

Fig. 1 Paramagnetic cosolvents used in this study. Gd(III)–DTPA–BMA or Omniscan provides 8 coordination sites for Gd(III) plus an inner-sphere water molecule, whereas the new probe, TTHA–TMA affords a total of 10 coordination sites for Gd(III)

Scheme 1 Synthesis of Gd(III)–TTHA–TMA paramagnetic cosolvent

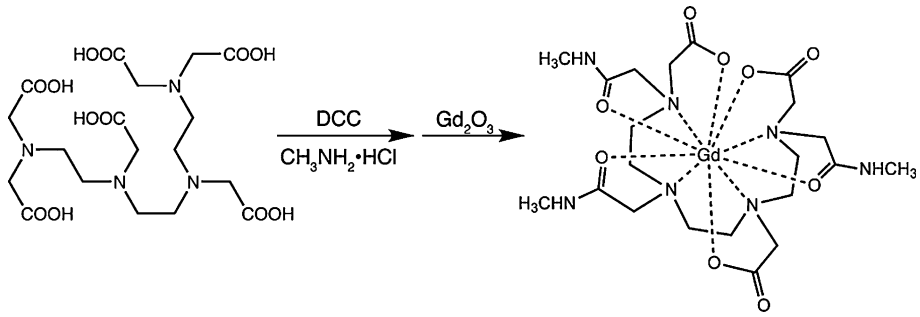

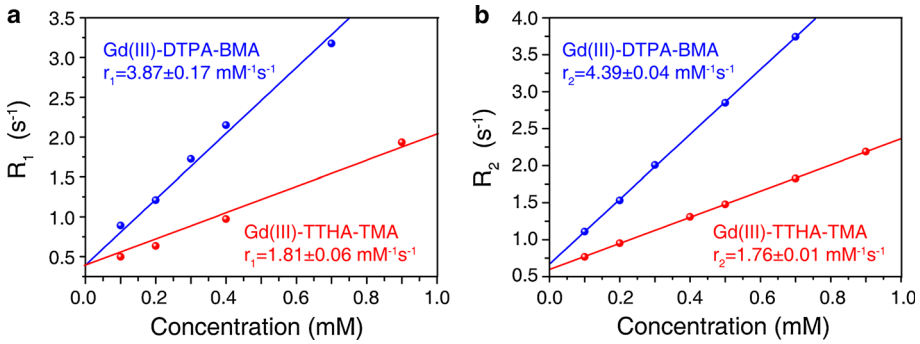

Fig. 2 Water relaxivity in the presence of Gd(III)–DTPA–BMA and Gd(III)–TTHA–TMA. **a** Longitudinal and **b** transverse relaxivities were measured for $^{1}H_2O$ at different concentrations of a paramagnetic cosolvent. The relaxivity is the slope obtained from linear regression. The extrapolated intercept at the Y-axis indicates intrinsic the water relaxation rate

We first assessed water relaxivity in the presence of the new probe. At unit concentration of the paramagnetic cosovlent, the longitudinal and transverse relaxivities are 1.81 ± 0.06 and 1.76 ± 0.01 mM^{-1} s^{-1} for Gd(III)–TTHA–TMA, respectively, less than half of the values for Gd(III)–DTPA–BMA (Fig. 2). The larger relaxivity for Gd(III)–DTPA–BMA is due to inner sphere water relaxation (Caravan et al. 1999), which is absent for Gd(III)–TTHA–TMA. The effectiveness and improvements of the new probe in sPRE measurement were then tested on three well-studied proteins.

With the addition of Gd(III)–TTHA–TMA paramagnetic cosolvent, we measured sPRE values for the protein GB1. Similar to water relaxivity, sPRE values for protein backbone amide scale linearly with the concentration of the paramagnetic cosovlent (Fig. S4). However, at high concentration of the cosolvent, some peaks start to broaden out and cannot be properly resolved from adjacent peaks. With the addition of 5 mM of the new probe, no residue was broadened out beyond detection and there was no drastic change in sPRE values between two consecutive residues (Fig. 3).

The sPRE value can be back calculated from the protein structure by integrating PRE contributions from all surrounding paramagnetic cosolvent molecules occupying in evenly spaced grid points (Hernandez et al. 2002; Pintacuda and Otting 2002). For each grid point, the sPRE value

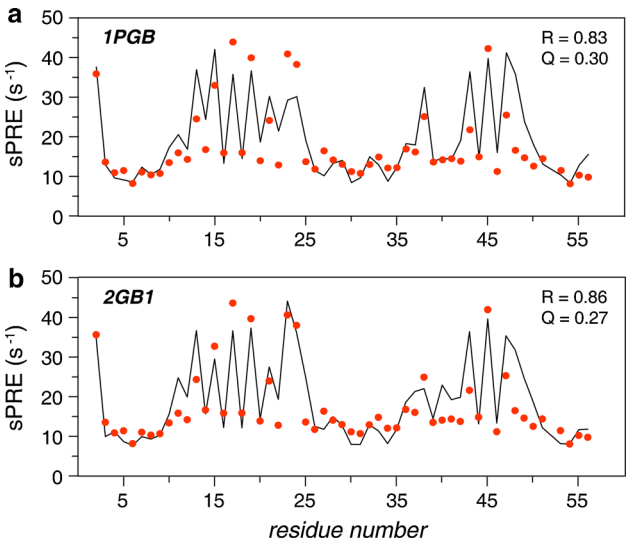

Fig. 3 sPRE values for protein GB1 with the addition of Gd(III)–TTHA–TMA cosolvent. Back calculated based on **a** X-ray structure 1PGB and **b** NMR structure 2GB1, respectively, the sPRE values are shown as *black lines*. The observed PRE values are shown as *orange spheres*. The correlation coefficients and PRE Q-factors after normalization are indicated

can be described by Solomon–Bloembergen equation (Solomon 1955; Solomon and Bloembergen 1956) following an $<r^{-6}>$ dependence on the depth of the nucleus.

The observed sPRE values agree well with the calculated values based on the X-ray and NMR structures of GB1 protein, namely 1PGB (Derrick and Wigley 1994) and 2GB1(Gronenborn et al. 1991) respectively. The agreement with the NMR structure, 2GB1, an averaged mean structure, is slightly better than that with the X-ray structure, 1PGB, affording correlation coefficient of 0.86 and 0.83, respectively.

The agreement in sPRE can also be assessed using PRE Q-factor (Iwahara et al. 2004). As the exact pre-factor for $<r^{-6}>$ dependence is related to the physical constants and probe concentration, normalization is performed by scaling the residue with the lowest sPRE value, Val54 in GB1. This residue has the deepest burial in the protein and therefore its sPRE can be back calculated most accurately. Upon normalization of the back calculated sPRE values, a process that does not affect correlation, the sPRE Q-factors are 0.30 and 0.27 for the PDB structures 1PGB and 2GB1, respectively. The largest differences in the calculated sPRE values based on the two known structures are at residues 23 and 24 (Fig. 3). Ala23 and Ala24 are both located near the N-terminal end of a GB1 helix. In the crystal structure (1PGB), the carboxylate group of Asp22 likely forms a hydrogen bond with the hydroxyl group of Thr25, and side chain of Asp22 sits on the top of the amide groups of Ala23 and Ala24 (Fig. S5). In the NMR structure (2GB1) however, the side chain of Asp22 swings away and the amide groups of Ala23 and Ala24 are more exposed (Fig. S5). Therefore, the sPRE measurement suggests the absence of a hydrogen bond between Asp22 and Thr25 in solution. On the other hand, high-quality sPRE data afforded with the new probe also makes small structural differences more obvious.

Gd(III)–TTHA–TMA was further evaluated on two other protein systems, enzyme EIIA^{Glc} from the phosphor-transferase system (PDB code for the crystal structure 1F3Z(Feese et al. 1997)) and MBP with a maltotriose bound (PDB code for the crystal structure 3MBP(Quiocho et al. 1997; Fig. S4). No peaks in EIIA^{Glc} were broadened out beyond detection upon addition of 5 mM paramagnetic cosolvent (Fig. 4). In contrast, upon addition of 4 mM Gd(III)–DTPA–BMA, residues Thr19, Glu72 and Gly102 disappeared, and Ser155 experience a very large sPRE. All these residues are located in a flexible region of the protein, with their amide protons pointing outwards and not hydrogen-bonded (Feese et al. 1997; Wang et al. 2000). Likewise, for the MBP, no residues are completely broadened out for the MBP, with the sPRE value ranging from 5 to 70 s^{-1}, with the addition of 5 mM Gd(III)–TTHA–TMA (Fig. S6).

In summary, we have developed a new paramagnetic cosolvent, Gd(III)–TTHA–TMA for the measurement of protein solvent PRE. This probe has a total of 10 coordination sites for a lanthanide ion, thus eliminating a water molecule bound at inner sphere. Free from water-transferred PRE, sPRE can be more reliably measured for a protein of interest, which information would aid protein structure determination. With this new probe, we envision sPRE shall facilitate the "structure" characterization of intrinsically disordered proteins that have a large number of labile protons.

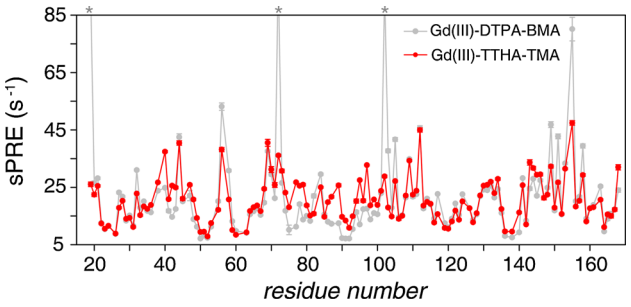

Fig. 4 sPRE profiles obtained for *E. coli* enzyme EIIA^{Glc} upon addition of either 4 mM Gd(III)–DTPA–BMA (colored in *grey*) or 5 mM Gd(III)–TTHA–TMA (colored in *red*). *Asterisks* denote residues that are broadened out beyond detection. *Lines* connect the residues simply for guiding the eyes. *Error bars* denote 1 standard deviation

Materials and methods

Synthesis of TTHA–TMA. Triethylene tetraamine hexaacetic acid (TTHA, 0.49 g, 1.0 mmol; purchased from Tokyo Chemical Industry) and triethylamine (TEA, 0.60 g, 6.0 mmol; purchased from Sinopharm Chemical Reagent) were dissolved in 10 ml acetonitrile. The solution was stirred at 60 °C for 1 h. Cooled in an ice bath, N,N'-dicyclohexylcarbodiimide (DCC, 0.72 g, 3.5 mmol; purchased from Sinopharm Chemical Reagent) was added to the solution, and the solution was stirred for another 0.5 h. Methylamine hydrochloride (0.24 g, 3.5 mmol; purchased from Sinopharm Chemical Reagent) and TEA (3.5 mmol, 0.35 g) were added to the solution, and the solution was stirred for 2 more hours. The ice bath was removed, and the reaction was allowed to proceed overnight at room temperature. After removing the precipitate through filtration, the solution was evaporated under vacuum, and the resulting white powder was used for the next step without further purification.

The obtained powder is a mixture of TTHA derivatives with various number of methyl amide groups, and was dissolved in 10 ml deionized water. Gd(III) oxide (0.16 g, 0.5 mmol; purchased from Acros Organics) was added to the solution and stirred overnight at 60 °C. Gd(III) oxide can only be solubilized when the constituting Gd(III) is

chelated with the TTHA derivatives, while the rest remains in the pellet and can be removed by filtration. The filtrate was further purified on Source-S and Source-Q columns, with the flow-through collected, thus affording only the product with no net charge, i.e. the gadolinium chelate of TTHA–TMA. The product was evaporated under vacuum to yield the desired paramagnetic cosolvent, triethylene tetraamine hexaacetate trimethylamide gadolinium chelate (Gd(III)–TTHA–TMA, 180 mg, 26 % yield). The product was confirmed by ESI–MS: calculated for $C_{21}H_{36}N_7O_9Gd$ [M + Na^+] 708.17, 709.17, 710.17, 711.17, 713.17, observed 708.18, 709.18, 710.18, 711.18, 713.18. There are multiple mass peaks arising from the 5 most abundant isotopes of gadolinium: ^{155}Gd, ^{156}Gd, ^{157}Gd, ^{158}Gd and ^{160}Gd.

Protein sample preparation. Both ^{15}N-labeled GB1 and $EIIA^{Glc}$ proteins were expressed in *E. coli* BL21-star cells and grown in isotope-enriched M9 minimum medium. Both proteins underwent purification through DEAE ion exchange fast-flow column, Superdex-100 size exclusion column, and Source-Q ion exchange column (GE Healthcare), in sequential order. The U–^{15}N,^{2}H-labeled MBP protein was expressed in the minimum medium prepared in $^{2}H_2O$, with ^{15}N–NH_4Cl and ^{13}C/^{2}H-glucose as the nitrogen and carbon sources and supplemented with 10 % (v/v) ^{15}N/^{13}C/^{2}H-Celltone (Silantes). MBP protein was purified over MBP–TRAP and Superdex-100 columns (GE Healthcare). To remove any bound ligand, the protein was denatured under 2 M Gnd–HCl and was refolded by desalting. All the proteins were concentrated and buffer-exchanged in the Amicon filter (Millipore) to be prepared in the NMR buffer: 20 mM pH 6.0 sodium acetate buffer (GB1), 20 mM pH 6.8 PIPES buffer ($EIIA^{Glc}$) or 20 mM pH 7.4 Tris–HCl buffer (MBP), all containing 100 mM NaCl. Protein concentration was 0.5 mM. For MBP, 5 mM maltotriose (Sigma) was added to ensure a *holo* state. In addition, 0.1 % NaN_3 and 10 % D_2O (v/v) were added to the NMR samples.

PRE experiments. NMR experiment was performed on 600 MHz Bruker spectrometer (for GB1 and $EIIA^{Glc}$) or 850 MHz (for MBP), both equipped with a cryogenic probe. Paramagnetic cosovlent of either Gd(III)–DTPA–BMA (GE Healthcare) or Gd(III)–TTHA–TMA was added to protein sample to a final concentration of 4 and 5 mM, respectively. The transverse PRE Γ_2 rates for backbone amide of protein GB1 were measured and analyzed using the standard protocol (Iwahara et al. 2004, 2007).

Back calculation of sPRE. A grid model was utilized for sPRE calculation, with the paramagnetic cosolvent evenly located at every grid point. The spacing of the grid is set to 0.2 Å, and the cut-off distance for PRE calculation is 40 Å, where PRE becomes negligible (Iwahara et al. 2004). Protein Cartesian coordinates are fixed and are padded with van der Waals radii of various nuclei. Grid points that are within protein structure plus the radius of paramagnetic cosolvent (4.0 Å for Gd(III)–TTHA–TMA and 3.5 Å for Gd(III)–DTPA–BMA) are excluded. The sPRE value for a particular protein nucleus is calculated using this equation

$$\Gamma_2 = k \sum_l \sum_m \sum_n w_{l,m,n} \cdot r_{l,m,n}^{-6}$$

in which k is a constant that are related to physical constants in the Solomon–Bloembergen equation (Solomon 1955; Solomon and Bloembergen 1956) and to the concentration of paramagnetic cosolvent. $r_{l,m,n}$ is the distance between grid point (l, m, n) and protein nucleus. $w_{l,m,n}$ is assigned to 1 if the paramagnetic probe can be placed at grid point (l, m, n), or 0 for excluded points. The back-calculated sPRE values are normalized to the lowest sPRE value (of the residue that is more deeply buried) when calculating PRE Q-factors (Iwahara et al. 2004).

Acknowledgments The work was supported by funds from the Ministry of Science and Technology of China (2013CB910200), the National Natural Sciences Foundation of China (21073230, 31170728 and 31125007), and Zhejiang Provincial Natural Science Foundation of China (Z2110059). C.T. is an international early career scientist of Howard Hughes Medical Institute (HHMI).

References

Berardi MJ, Shih WM, Harrison SC, Chou JJ (2011) Mitochondrial uncoupling protein 2 structure determined by NMR molecular fragment searching. Nature 476:109–113

Bernini A, Venditti V, Spiga O, Niccolai N (2009) Probing protein surface accessibility with solvent and paramagnetic molecules. Prog Nucl Magn Reson Spectrosc 54:278–289

Caravan P, Ellison JJ, McMurry TJ, Lauffer RB (1999) Gadolinium(III) chelates as MRI contrast agents: structure, dynamics, and applications. Chem Rev 99:2293–2352

Clore GM, Iwahara J (2009) Theory, practice, and applications of paramagnetic relaxation enhancement for the characterization of transient low-population states of biological macromolecules and their complexes. Chem Rev 109:4108–4139

Derrick JP, Wigley DB (1994) The third IgG-binding domain from streptococcal protein G. An analysis by X-ray crystallography of the structure alone and in a complex with Fab. J Mol Biol 243:906–918

Eliezer D (2012) Distance information for disordered proteins from NMR and ESR measurements using paramagnetic spin labels. Methods Mol Biol 895:127–138

Feese MD, Comolli L, Meadow ND, Roseman S, Remington SJ (1997) Structural studies of the Escherichia coli signal transducing protein IIAGlc: implications for target recognition. Biochemistry 36:16087–16096

Gillespie JR, Shortle D (1997) Characterization of long-range structure in the denatured state of staphylococcal nuclease. I. Paramagnetic relaxation enhancement by nitroxide spin labels. J Mol Biol 268:158–169

Gottstein D, Reckel S, Dotsch V, Guntert P (2012) Requirements on paramagnetic relaxation enhancement data for membrane protein structure determination by NMR. Structure 20:1019–1027

Gronenborn AM, Filpula DR, Essig NZ, Achari A, Whitlow M, Wingfield PT, Clore GM (1991) A novel, highly stable fold of the immunoglobulin binding domain of streptococcal protein G. Science 253:657–661

Guttler T, Madl T, Neumann P, Deichsel D, Corsini L, Monecke T, Ficner R, Sattler M, Gorlich D (2010) NES consensus redefined by structures of PKI-type and Rev-type nuclear export signals bound to CRM1. Nat Struct Mol Biol 17:1367–1376

Hernandez G, Teng CL, Bryant RG, LeMaster DM (2002) O2 penetration and proton burial depth in proteins: applicability to fold family recognition. J Am Chem Soc 124:4463–4472

Iwahara J, Schwieters CD, Clore GM (2004) Ensemble approach for NMR structure refinement against (1)H paramagnetic relaxation enhancement data arising from a flexible paramagnetic group attached to a macromolecule. J Am Chem Soc 126:5879–5896

Iwahara J, Zweckstetter M, Clore GM (2006) NMR structural and kinetic characterization of a homeodomain diffusing and hopping on nonspecific DNA. Proc Natl Acad Sci USA 103:15062–15067

Iwahara J, Tang C, Clore GM (2007) Practical aspects of 1H transverse paramagnetic relaxation enhancement measurements on macromolecules. J Magn Reson 184:185–195

Karaca E, Bonvin AM (2013) Advances in integrative modeling of biomolecular complexes. Methods 59:372–381

Keizers PH, Mersinli B, Reinle W, Donauer J, Hiruma Y, Hannemann F, Overhand M, Bernhardt R, Ubbink M (2010) A solution model of the complex formed by adrenodoxin and adrenodoxin reductase determined by paramagnetic NMR spectroscopy. Biochemistry 49:6846–6855

Klammt C, Maslennikov I, Bayrhuber M, Eichmann C, Vajpai N, Chiu EJ, Blain KY, Esquivies L, Kwon JH, Balana B, Pieper U, Sali A, Slesinger PA, Kwiatkowski W, Riek R, Choe S (2012) Facile backbone structure determination of human membrane proteins by NMR spectroscopy. Nat Methods 9:834–839

Koehler J, Meiler J (2011) Expanding the utility of NMR restraints with paramagnetic compounds: background and practical aspects. Prog Nucl Magn Reson Spectrosc 59:360–389

Madl T, Bermel W, Zangger K (2009) Use of relaxation enhancements in a paramagnetic environment for the structure determination of proteins using NMR spectroscopy. Angew Chem Int Ed Engl 48:8259–8262

Madl T, Guttler T, Gorlich D, Sattler M (2011) Structural analysis of large protein complexes using solvent paramagnetic relaxation enhancements. Angew Chem Int Ed Engl 50:3993–3997

Mal TK, Ikura M, Kay LE (2002) The ATCUN domain as a probe of intermolecular interactions: application to calmodulin-peptide complexes. J Am Chem Soc 124:14002–14003

Otting G (2010) Protein NMR using paramagnetic ions. Annu Rev Biophys 39:387–405

Petros AM, Mueller L, Kopple KD (1990) NMR identification of protein surfaces using paramagnetic probes. Biochemistry 29:10041–10048

Pintacuda G, Otting G (2002) Identification of protein surfaces by NMR measurements with a paramagnetic Gd(III) chelate. J Am Chem Soc 124:372–373

Quiocho FA, Spurlino JC, Rodseth LE (1997) Extensive features of tight oligosaccharide binding revealed in high-resolution structures of the maltodextrin transport/chemosensory receptor. Structure 5:997–1015

Schwieters CD, Kuszewski JJ, Clore GM (2006) Using Xplor-NIH for NMR molecular structure determination. Prog Nucl Magn Reson Spectrosc 48:47–62

Solomon I (1955) Relaxation processes in a system of two spins. Phys Rev 99:559–565

Solomon I, Bloembergen N (1956) Nuclear magnetic interactions in the Hf molecule. J Chem Phys 25:261–266

Venditti V, Niccolai N, Butcher SE (2008) Measuring the dynamic surface accessibility of RNA with the small paramagnetic molecule TEMPOL. Nucleic Acids Res 36:e20

Wang G, Louis JM, Sondej M, Seok YJ, Peterkofsky A, Clore GM (2000) Solution structure of the phosphoryl transfer complex between the signal transducing proteins HPr and IIA(glucose) of the Escherichia coli phosphoenolpyruvate:sugar phosphotransferase system. EMBO J 19:5635–5649

Wang Y, Schwieters CD, Tjandra N (2012) Parameterization of solvent-protein interaction and its use on NMR protein structure determination. J Magn Reson 221:76–84

Wüthrich KW (1986) NMR of proteins and nucleic acids. Wiley, New York